Luminol Activity of Horseradish Peroxidase Mutants Mimicking a Proposed Binding Site for Luminol in *Arthromyces ramosus* Peroxidase[†]

Motomasa Tanaka,[‡,§] Koichiro Ishimori, and Isao Morishima*

Department of Molecular Engineering, Graduate School of Engineering, Kyoto University, Kyoto 606-8501, Japan

Received March 30, 1999; Revised Manuscript Received June 7, 1999

ABSTRACT: To enhance the oxidation activity for luminol in horseradish peroxidase (HRP), we have prepared three HRP mutants by mimicking a possible binding site for luminol in *Arthromyces ramosus* peroxidase (ARP) which shows 500-fold higher oxidation activity for luminol than native HRP. Spectroscopic studies by ^{1}H NMR revealed that the chemical shifts of 7-propionate and 8-methyl protons of the heme in cyanide-ligated ARP were deviated upon addition of luminol (4 mM), suggesting that the charged residues, Lys49 and Glu190, which are located near the 7-propionate and 8-methyl groups of the heme, are involved in the specific binding to luminol. The positively charged Lys and negatively charged Glu were introduced into the corresponding positions of Ser35 (S35K) and Gln176 (Q176E) in HRP, respectively, to build the putative binding site for luminol. A double mutant, S35K/Q176E, in which both Ser35 and Gln176 were replaced, was also prepared. Addition of luminol to the HRP mutants induced more pronounced effects on the resonances from the heme substituents and heme environmental residues in the ^{1}H NMR spectra than that to the wild-type enzyme, indicating that the mutations in this study induced interactions with luminol in the vicinity of the heme. The catalytic efficiencies (V_{max}/K_m) for luminol oxidation of the S35K and S35K/Q176E mutants were 1.5- and 2-fold improved, whereas that of the Q176E mutant was slightly depressed. The increase in luminol activity of the S35K and S35K/Q176E mutants was rather small but significant, suggesting that the electrostatic interactions between the positive charge of Lys35 and the negative charge of luminol can contribute to the effective binding for the luminol oxidation. On the other hand, the negatively charged residue would not be so crucial for the luminol oxidation. The absence of drastic improvement in the luminol activity suggests that introduction of the charged residues into the heme vicinity is not enough to enhance the oxidation activity for luminol as observed for ARP.

Heme-containing peroxidases distributed in various plants and animal tissues perform important physiological roles by oxidation reactions with a wide variety of organic and inorganic substrates. In the catalytic cycle of heme peroxidase, the ferric resting enzyme reacts with hydrogen peroxide (H_2O_2) as an oxidant to yield an active intermediate called compound I, in which 2 oxidation equiv are stored as a ferryl species and a porphyrin π cation radical (*1*). Compound I is reduced back to the resting state via the second intermediate, compound II, which is concomitant with oxidation of two substrate molecules. One of the most intensively studied members of this enzyme superfamily is horseradish peroxidase (HRP).[1] HRP is an extracellular plant enzyme involved in regulation of cell growth and differentiation, polymerization of cell wall components, and oxidation of secondary metabolites essential for certain pathogenic defense reactions (*2*).

In addition to these functions in the biological systems, the oxidation reaction of luminol mediated by HRP has long been utilized in immunoassays to detect and quantitate the analytes bound to HRP by chemiluminescence (*3*). Although the detection system based on the oxidation by HRP has been established and widely used for clinical examinations, one disadvantage of the conventional chemiluminescence assay is the inefficiency of the luminescence reaction due to its low quantum yield in comparison with that of the bioluminescence assay. To detect and quantitate smaller amounts of the analytes in clinical tests, a lot of effort has been devoted to enhance the luminol activity of HRP (*4*). Recently, one of the heme-containing peroxidases, *Arthromyces ramosus* peroxidase (ARP), isolated from the hypomycete *Arthromyces ramosus* (fungi imperfecti) was found to show

[†] This work was supported in part by grants-in-aid for scientific research on priority areas "Molecular Biometallics" (08249102 to I. M.) from the Ministry of Education, Science, Culture and Sports.

* To whom correspondence should be addressed. (Phone) +81-75-753-5921; (fax) +81-75-751-7611; (e-mail) morisima@mds.moleng.kyoto-u.ac.jp.

[‡] Supported by Research Fellowships of the Japan Society for the Promotion of Science for Young Scientists.

[§] Present address: Brain Science Institute, The Institute of Physical and Chemical Research (RIKEN), 2-1 Hirosawa, Wako, Saitama 351-0198, Japan.

[1] Abbreviations: HRP, horseradish peroxidase isozyme C; native HRP, peroxidase isolated from horseradish, isoenzyme C; wild-type, recombinant horseradish peroxidase isozyme C expressed in *Escherichia coli*; ARP, *Arthromyces ramosus* peroxidase; ABTS, 2,2′-azidobis(3-ethylbenzothiazoline-6-sulfonic acid)diammonium salt; ARP-CN, cyanide-ligated *Arthromyces ramosus* peroxidase; HRP-CN, cyanide-ligated horseradish peroxidase isozyme C; CIP, *Coprinus cinereus* peroxidase; MnP, manganese peroxidase; BHA, benzhydroxamic acid.

10.1021/bi9907328 CCC: $18.00
Published on Web 07/23/1999

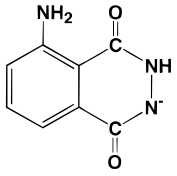

FIGURE 1: Chemical structure of luminol.

500-fold higher oxidation activity for luminol than HRP (*5*). Since the prominent enhancement in the oxidation activity of ARP is characteristic of luminol, and not observed for other aromatic substrates (*5*), ARP has been expected to have a specific binding site for luminol. Although the X-ray crystal structure of ARP has not yet identified the binding site for luminol, the remarkable increase in oxidation activity for luminol prompted us to develop a more sensitive detection system of chemiluminescence based on HRP by mimicking a possible binding site for luminol in ARP.

In the present study, to estimate the binding site for luminol in ARP, we have examined circular dichroism (CD) and nuclear magnetic resonance (NMR) spectra of ARP before and after addition of luminol. Together with differences of the X-ray crystal structures between ARP and HRP, the spectral changes induced by addition of luminol suggested that a region surrounded by Lys49, Glu190, 7-propionate, and 8-methyl groups of the heme in the distal site of ARP is involved in the binding site for luminol. Since the charged residues, Lys49 and Glu190, are substituted for noncharged residues, Ser35 and Gln176 in HRP, respectively, it is likely that electrostatic interactions between the side chains of Lys49 and Glu190 and the polar functional groups of luminol (Figure 1) improve the affinity for luminol, resulting in enhancement of the oxidation activity of ARP.

To enhance the luminol activity of HRP, we have prepared ARP-type HRP mutants, S35K and Q176E, by replacing Ser35 and Gln176 with Lys and Glu, respectively. To mimic the putative binding site for luminol in ARP more accurately, a double mutant, S35K/Q176E, in which both Ser35 and Gln176 were replaced, was also expressed. In addition, S35A (Ser35 → Ala) and Q176A (Gln176 → Ala) mutants were constructed as negative controls, in which a hydrophobic residue, alanine, was introduced, instead of the charged residues. The structural properties of the five HRP mutants (S35K, Q176E, S35K/Q176E, S35A, and Q176A) were investigated by various spectroscopic techniques including CD, NMR, and resonance Raman. The steady-state kinetics, elementary reaction rates, and redox potentials were also examined to characterize the catalytic activity of the HRP mutants, and these results were compared with those of ARP.

EXPERIMENTAL METHODS

Materials. ARP was provided by Suntory Ltd., Japan. Native HRP (type VI), predominantly isozyme C, was purchased from Sigma as a lyophilized, desalted powder and used without further purification. The A_{402}/A_{280} ratio (RZ value) of ARP and native HRP is 2.7 and 3.2, respectively. ^{15}N-enriched K^{15}N was purchased from Cambridge Isotope Laboratories. General molecular biology supplies were obtained from Takara and Perkin-Elmer. General organic and inorganic compounds were purchased from Wako Pure Chemical Industries and Nacalai Tesque as the highest quality available.

Expression and Purification of Recombinant HRPs. Site-directed mutagenesis was performed by using T7 expression vector constructed by Nagano et al. (*6*). Double-stranded DNA sequence analysis with 373 DNA sequencer (Applied Biosystems) verified introduction of the mutation without additional mutations in the whole HRP-coding gene.

The wild-type and mutant HRPs were expressed in *Escherichia coli* (BL21 strain), and apoHRP was extracted from the inclusion bodies as previously reported (*6*). Reactivation of apoHRP with heme in the presence of calcium ion and purification of holoHRP were described elsewhere (*7*). RZ values of purified wild-type and mutant HRPs were about 3.2 and 3.3, respectively. The concentration of peroxidase was estimated by the extinction coefficient determined in the pyridine hemochrome forms of the enzyme. (*8*). The extinction coefficients were 108, 102, 103, 102, 103, 102, 101, and 112 $mM^{-1}\cdot cm^{-1}$ for ARP, native HRP, wild-type HRP, S35K, S35A, Q176E, Q176A, and S35K/Q176E mutants, respectively.

Circular Dichroism (CD) Spectroscopy. CD spectra of ARP and HRPs in the Soret and far-UV regions were measured with JASCO J-720 at ambient temperature. ARP and HRPs were dissolved in 50 mM sodium phosphate buffer at pH 7.0, with or without luminol (4 mM). Mean residue α-helical content was evaluated from the molar ellipticity at 222 nm by following eq 1 (*9*):

$$\alpha\text{-helix}\ (\%) = \{-([\theta]_{222} + 2340)/30300\} \times 100 \quad (1)$$

CD spectra were an average of 16 scans recorded at a speed of 100 nm/min and a resolution of 0.2 nm. Light paths of the observing cells were 10 mm for measurements in the Soret region and 1 mm in the far-UV region.

Resonance Raman Spectroscopy. Resonance Raman spectra of HRPs were recorded with excitation from a Kr^+ ion laser (Spectra Physics, Model 2060) and He/Cd laser (Kinmon Electrics, Model CD 1805B) using the 406.7 and 441.6 nm line, respectively. The resonance Raman scattering was detected with a charge-coupled device (CCD) (Astromed CCD3200) attached to a single polychromator (Ritsu Oyo Kogaku, DG-1000). Sample solutions were sealed in a spinning quartz cells cooled by flushing cold nitrogen gas. The spectral slit width was set to 100 μm throughout the experiments. The calibration of the Raman line was performed with indene (1300−1700 cm^{-1}) or carbon tetrachloride (200−400 cm^{-1}) as a standard. Ferrous HRPs were prepared by adding small amounts of freshly saturated sodium dithionite solution to the degassed ferric enzyme solutions.

Nuclear Magnetic Resonance (NMR) Spectroscopy. ^{1}H NMR measurements were performed on a BRUKER Avance DRX500 spectrometer. ^{1}NMR spectra were recorded at 23.0 (ARP and native HRP) or 17.0 °C (wild-type and mutant HRPs) using a temperature control unit of the spectrometer. A LOSAT pulse sequence was employed with a 64 000 data transform of 150 kHz and a 8.5 μs 90° pulse. The concentration of cyanide-ligated ARP (ARP-CN) and HRPs (HRPs-CN) was ca. 500 μM on a heme basis in 90% H_2O/10% ^2H_2O containing 50 mM sodium phosphate buffer at pH 7.0, with or without luminol (4 mM). Peak shifts were referenced to the residual water signal which is calibrated against tetramethylsilane (TMS). ^{15}N NMR spectra of C^{15}N-ligated

ARP and native HRP were aquired at 50.67 MHz. Chemical shifts are given with reference to the resonance of external $^{15}NH_3$. Sample conditions for the ^{15}N NMR spectra were the same as those for ^1H NMR spectra except for the concentration of the enzymes (1 mM).

Peroxidase Activities under Steady-State Conditions. Steady-state kinetic constants for luminol oxidation were obtained by measuring the absorbance change at 500 nm on a Shimadzu UV-2200 spectrophotometer at 25 °C. The final concentrations of HRPs and ARP are 20 and 1 nM, respectively. The solution contains 50 mM sodium phosphate buffer at pH 7.0, 0.5 mM H_2O_2, and 1−10 mM (for HRPs) or 0.05−0.4 mM (for ARP) luminol. For hydroquinone oxidation, a HRP or ARP (∼0.2 μM) solution was added to a cuvette containing 0.5 mM H_2O_2 and 100−1600 μM (for HRPs) or 200−3200 μM (for ARP) hydroquinone in 50 mM sodium phosphate buffer at pH 7.0 to a final concentration of 1 nM. The initial oxidation rate was calculated by the absorbance change at 250 nm monitored on a Shimadzu UV-2200 spectrophotometer at 25 °C. For ABTS [2,2′-azidobis-(3-ethylbenzothiazoline-6-sulfonic acid) diammonium salt] oxidation, 10 μL of a 0.4 mM HRP or ARP solution was added to a 2 mL solution containing 1.0 mM H_2O_2 and 100−1600 μM (for HRPs) or 12.5−800 μM (for ARP) ABTS in 50 mM sodium phosphate buffer at pH 6.0. The final concentration of the protein was 2 nM. The initial oxidation rate was determined by following the increase in the absorbance at 405 nm at 25 °C. The initial oxidation rates were expressed as mM·min^{-1} by using the molar absorption coefficients of the oxidation products of hydroquinone (8.28 mM^{-1}·cm^{-1}) (*10*) and ABTS (36.8 mM^{-1}·cm^{-1}) (*11*). Kinetic parameters, K_m and V_{max}, were obtained from the initial oxidation rates, k_{int}, and the concentration of substrate, [S], using eq 2:

$$k_{int} = V_{max}[S]/(K_m + [S]) \quad (2)$$

Elementary Reaction Rates in the Catalytic Cycle. Formation (k_1) and reduction (k_2) rates of compound I and the reduction rate (k_3) of compound II under pseudo-first-order conditions were measured on a spectrophotometer (OLIS, USA) equipped with a stopped-flow mixer (Unisoku, Japan) at 25 °C in 50 mM sodium phosphate buffer, pH 7.0. More than 10-fold excess of H_2O_2 or substrate such as luminol and guaiacol relative to the concentration of HRP or ARP (2.0 μM) was utilized to ensure pseudo-first-order kinetics. The elementary reaction rates of k_1, k_2, and k_3 were determined by the absorbance changes at 395, 412, and 424 nm, respectively.

Reduction Potentials of Compounds I and II. Reduction potentials of compounds I and II were measured from redox equilibria of HRP with iridate according to the method by Hayashi and Yamazaki (*12*). Five microliters of 4 mM K_2IrCl_6 containing 0.01 M HCl was added to 2 mL of 10 μM HRP solution in 50 mM sodium phosphate buffer at pH 7.0. The mixture was allowed to be equilibrated for 20 min at 4.0 °C. The concentrations of ferric HRP, compounds I and II, and K_2IrCl_6 in the equilibrium were calculated by deconvolution of the UV−visible spectrum of the mixture into four respective authentic UV−visible spectra. The concentration of K_3IrCl_6 in the equilibrium was estimated by subtracting the concentration of K_2IrCl_6 in the equilibrium from that of initially added K_2IrCl_6. The reduction potentials of compounds I and II were determined using the concentrations of each component in the equilibrium, the Nernst equation, and a value of 0.90 V for $E_0'(K_2IrCl_6/K_3IrCl_6)$ (*10*). All reduction potentials reported herein are referenced *vs.* NHE.

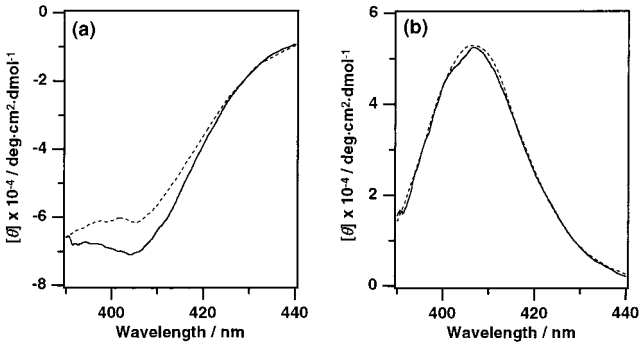

FIGURE 2: CD spectra in the Soret region of ferric (a) ARP and (b) native HRP in sodium phosphate buffer, pH 7.0. The dashed and solid lines show the spectra before and after addition of luminol (4 mM), respectively.

RESULTS AND DISCUSSION

CD Spectra of ARP and Native HRP. Although the heme prosthetic group is not optically active, the circular dichroism (CD) is induced by coupled oscillator interactions between allowed electronic transition moments of the porphyrin ring and those of neighboring aromatic residues in the heme pocket (*13*). In Figure 2, the CD spectra of ARP and native HRP in the absence and presence of luminol (4 mM) are presented. The negative molar ellipticities observed in the spectrum of ARP were definitely decreased upon addition of luminol [Figure 2(a)], reflecting the significant changes in the interactions between the heme chromophore and environmental amino acid residues, probably due to the accessibility of luminol to the heme cofactor. In sharp contrast to the negative ellipticity and prominent spectral changes by luminol in ARP, the CD spectra of native HRP show a positive ellipticity, which was insensitive to addition of luminol [Figure 2(b)]. No substantial changes in the spectrum of HRP suggest that the weak affinity of luminol to native HRP is due to the absence of the specific binding site and/or that structural changes in the heme environment upon addition of luminol are quite small.

^1H and ^{15}N NMR Spectra of ARP and Native HRP. Structural changes of the heme environment induced by addition of luminol were supported by ^1H NMR spectra of the cyanide-ligated peroxidases. Although the cyanide-ligated form of peroxidase is inactive for the catalytic reaction, the ^1H NMR spectra of the cyanide adducts show well-resolved proton resonances, which allow us to examine not only the electronic state of the heme but also the configuration of several amino acid residues surrounding the heme group. Figure 3(a) displays ^1H NMR spectra of ARP-CN in the absence (dashed line) and presence (solid line) of luminol (4 mM). As clearly shown in the spectra, three resonances (A, B, and C) exhibited slight but significant shifts by addition of luminol. Although the complete signal assignments in ARP have not yet been done, peak A can be assigned to the 8-methyl group of the heme with reference to the ^1H NMR spectrum of cyanide-ligated *Coprinus*

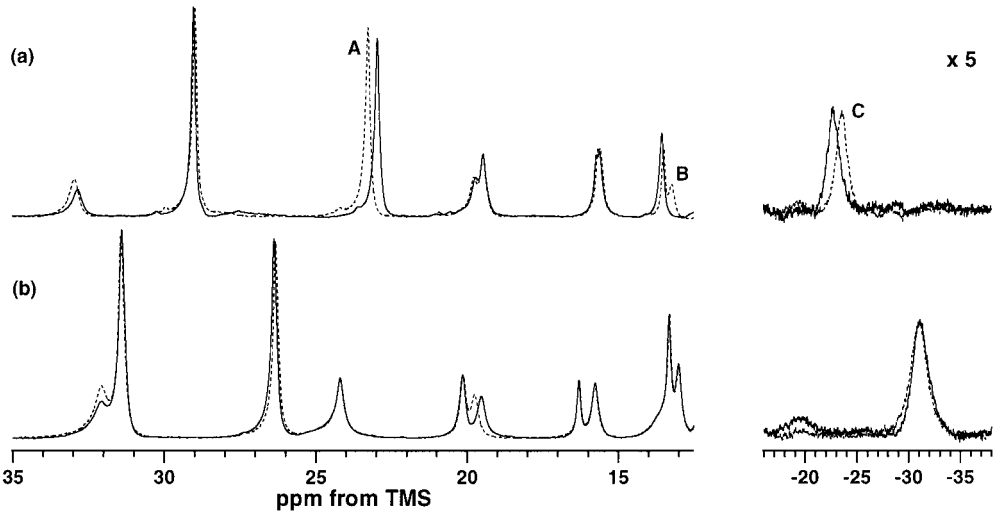

FIGURE 3: ^{1}H NMR spectra in the hyperfine-shifted region of cyanide-ligated (a) ARP and (b) native HRP in 90% H_2O/10% ^2H_2O sodium phosphate buffer, pH 7.0 at 23.0 °C. The dashed and solid lines show the spectra before and after addition of luminol (4 mM), respectively.

cinereus peroxidase (CIP) (*14*), which is identical to ARP except for the glycosylation patterns (*15*). In addition, the NOE connectivity with peak A in a NOESY spectrum of ARP-CN (data not shown) indicates that peak B is derived from the 7-propionate H_α. Since the pseudocontact shift of the proton resonance is amenable to the heme environmental structure (*16*), the specific shifts of peaks A and B upon addition of luminol suggest that luminol binds in close proximity to the 7-propionate and 8-methyl groups of the heme in ARP. However, a previous study pointed out that changes in pseudocontact shifts can be observed for protons far from the structural perturbation (*17*). We cannot completely exclude possibilities for the other luminol binding site. To gain further insights into the binding site for luminol in ARP, we measured a NOESY spectrum of ARP-CN in the presence of luminol (10 mM). However, we could not observe clear NOE connectivities between amino acid residues and luminol in the NOESY spectrum of ARP-CN due to the low solubility of luminol in the buffer and/or the fast exchange of luminol between bound and unbound forms.

Another signal perturbed by addition of luminol (peak C) was observed in the upfield region, which can be assigned to the proton resonance of $C_\epsilon H$ in the proximal His (*18*). Although the notable upfield shift for this resonance might reflect conformational changes around the proximal His, the resonance positions of the proximal His $C_\beta H$ at 19.5 and 15.6 ppm, which were assigned by the NOESY spectrum (data not shown), were insensitive to addition of luminol, suggesting that the proximal structure was not perturbed seriously. Since the previous analysis for the ^{1}H NMR hyperfine shift pattern of HRP-CN has revealed that the resonance position of $C_\epsilon H$ in the proximal His depends on the orientation of the heme magnetic axes (*19*), it is more likely that the binding of luminol in the distal site affected the configuration of the heme-bound cyanide, resulting in the shift of the proximal histidyl $C_\epsilon H$.

For native HRP-CN, luminol induced quite minor spectral changes [Figure 3(b)]. The resonance positions of the 8-methyl group of the heme and the proximal histidyl $C_\epsilon H$, which are sensitive to binding of luminol in ARP, were almost independent of addition of luminol, whereas only the resonance position of the peak at 19.6 ppm was perturbed, which has been assigned to the 7-propionate H_α of the heme (*18*). The signal was shifted to the upfield region by 0.2 ppm in the presence of luminol, implying that luminol also approaches near the 7-propionate of the heme in HRP as well as in ARP, but the smaller shift might correspond to the low binding affinity of HRP for luminol and/or the structural perturbation by luminol binding in the heme periphery would be small in HRP.

Table 1: ^{15}N Chemical Shifts (ppm from NH_3) of ARP−C^{15}N and Native HRP−C^{15}N at 17.0 °C

peroxidase	−luminol	+luminol
ARP	967	977
HRP	975	973

To dissect the effects of luminol on the distal side of the heme, ^{15}N NMR spectra of ARP-CN and HRP-CN were also aquired (spectra are not shown), since the ^{15}N chemical shift of the heme-bound C^{15}N is one of the sensitive indicators for structural perturbations around the distal His[2] (*20*). A resonance of the heme-bound C^{15}N in ARP-CN was observed at 967 ppm (Table 1). Addition of luminol (4 mM) to ARP-CN caused a large shift to the low field by 10 ppm. Such a low-field shift of the C^{15}N signal was also reported when the steric hindrance around the heme-bound cyanide was increased in the model complex (*21*), supporting the binding site of luminol in the distal site of ARP. On the other hand, only a slight upfield shift (2 ppm) was detected for HRP-CN (Table 1), which also suggests the weaker binding of luminol in HRP.

Possible Binding Site for Luminol. The present ^{1}H and ^{15}N NMR spectra, therefore, allow us to propose that luminol binds near the 7-propionate and 8-methyl groups of the heme in the distal site of ARP. However, comparison of the heme environmental structure between ARP and HRP has revealed that the relative positions of these heme substituents to the backbone structure of ARP are almost identical to those of

[2] Another factor determining the chemical shift of heme-bound C^{15}N is the basicity of the proximal His (*39*). However, perturbation on the basicity of the proximal His in ARP upon the binding of luminol would be small, since two resonance positions of the proximal histidyl $C_\beta H$ were not affected by the addition of luminol (Figure 3).

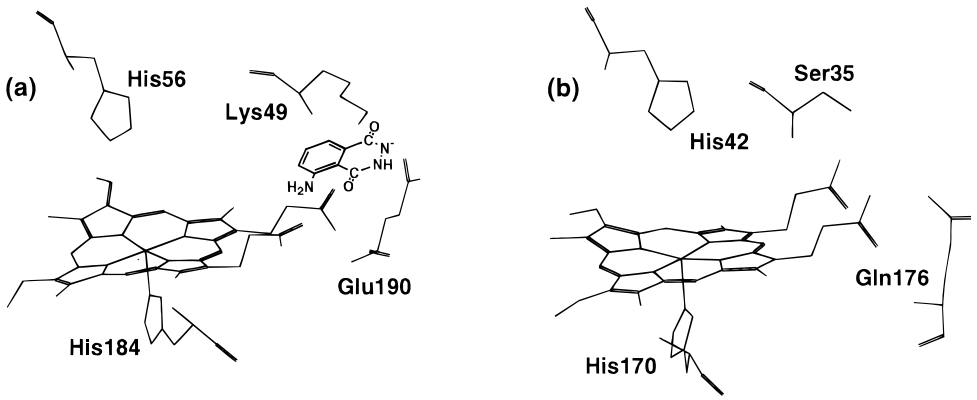

FIGURE 4: Heme environmental structure of (a) ARP and (b) HRP. Lys49 and Glu190 in ARP correspond to Ser35 and Gln176 in HRP, respectively (*21, 22*). One of the possible binding modes of luminol is shown at the proposed binding site in ARP (a).

Table 2: Amino Acid Sequences of ARP and HRP

peroxidase	amino acid sequence
ARP	^{47}VR**K**IL^{51}.....^{188}SQ**E**GL^{192}
HRP	^{33}AA**S**IL^{37}.....^{174}KN**Q**CR^{178}

[a] The amino acid residues in boldface characters are highlighted in this study. Comparison of the amino acid sequences is based on reference *22*.

HRP, which would exclude the possibility that the specific binding site for luminol is characterized by the relative positions of the heme substituents in ARP.

It should be noted here that ARP shows a much higher oxidation activity for luminol than for other aromatic substrates including typical substrates, phenols (*5*). As illustrated in Figure 1, the structure of luminol can be characterized by the several positively and negatively charged substituents at the periphery of the ring, which differentiates luminol from other aromatic substrates. On the basis of the X-ray crystal structure near the proposed binding site of ARP, we found that charged residues, Lys49 and Glu190, are located in the vicinity of the 7-propionate and 8-methyl groups of the heme in the distal site of ARP (*22*), which would fix luminol near the heme moiety by electrostatic interactions with the carbonyl oxygen and amino groups of luminol. The charged amino acid residues in ARP, Lys49 and Glu190, are replaced with noncharged residues in HRP, Ser35 and Gln176, respectively (*23*) (Figure 4, Table 2), resulting in the lack of electrostatic interactions with luminol.

The putative binding site for luminol near the 7-propionate and 8-methyl groups of the heme and interactions with nearby amino acid residues would also be supported by the recent X-ray crystal structure of the ARP complex with an aromatic substrate, benzhydroxamic acid (BHA). Although relatively low oxidation reactivity for BHA by ARP might still suggest a different binding site of luminol from that of BHA, the structural similarity of BHA to the aromatic ring of luminol allows us to speculate that some of the interactions for the binding of BHA are common with those of luminol. In the X-ray crystal structure, the aromatic ring of BHA is almost parallel to the heme plane and located near the 8-methyl group of the heme in the distal pocket, and the functional polar groups (CO, NH, OH) of BHA are directed to the heme iron by the hydrogen bonds to His56 (distal His) N_ϵ, Arg52 N_ϵ, and Pro154 O (*24*). Thus, we can propose that the position of the aromatic ring in luminol would also be superimposed with that of BHA and that the polar substituents of luminol electrostatically interact with the charged residues, Lys49 and Glu190, in close proximity to the 7-propionate and 8-methyl groups of the heme, as shown in Figure 4.

The substrate binding site near the 7-propionate and 8-methyl groups of the heme is not specific to ARP, but common to several peroxidases. Manganese peroxidase (MnP) binds its substrate, Mn^{2+} ion, by coordination of the 7-propionate of the heme, Glu35, Gln39, and Asp179 (*25*). Glu35, Glu39, and Asp179 in MnP correspond to Ser45, Lys49, and Glu190 in ARP, respectively, which are included in the proposed binding site for luminol. In HRP, Veitch et al. recently found by ^{1}H NMR spectroscopy that Phe179, which is located adjacent to the proposed binding site for luminol in ARP, is related to the binding of aromatic substrates (*26*). The previous inactivation studies on HRP by phenylhydrazine also revealed that the oxidation reaction occurs near the δ-meso carbon of the heme (*27*). Other evidence that substrates are bound near the proposed binding site is provided by the observation of NOEs between substrate molecules such as resorcinol and *p*-cresol, and the 8-methyl group of the heme in HRP (*28, 29*). These results suggest that the 7-propionate and 8-methyl groups of the heme constitute the core of the binding site for substrate. Therefore, the substrate specificity of peroxidase would depend on amino acid residues in the vicinity of the 7-propionate and 8-methyl groups of the heme. Since Lys49 and Glu190 are specific to ARP, not found for other peroxidases, these charged amino acid residues are likely responsible for the preferential high affinity for luminol in ARP.

Design of ARP-Type HRP Mutants. To enhance the oxidation activity for luminol of HRP, we have prepared three ARP-type HRP mutants by introducing the charged residue in the proposed binding site for luminol of ARP into HRP. Ser35 and Gln176 in HRP were replaced with the corresponding residues in ARP, Lys (S35K) and Glu (Q176E), respectively. To mimic the putative binding site for luminol more accurately, a double mutant, S35K/Q176E, in which both Ser35 and Gln176 are substituted, was also prepared. As the negative controls, S35A (Ser35 → Ala) and Q176A (Gln176 → Ala) mutants were also constructed. The structural and catalytic features of the five HRP mutants (S35K, S35A, Q176E, Q176A, and S35K/Q176E) were

Table 3: Mean Residue Molar Ellipticities at 222 nm and Estimated α-Helical Contents of Ferric Wild-Type, S35K, S35A, Q176E, Q176A, and S35K/Q176E HRPs

HRP	$-[\theta]_{222} \times 10^{-4}$ [a]	α-helix (%)
wild-type	1.40	39
S35K	1.48	41
S35A	1.45	40
Q176E	1.51	42
Q176A	1.47	41
S35K/Q176E	1.45	40

[a] Mean residue ellipticity in deg·cm^2·dmol^{-1}.

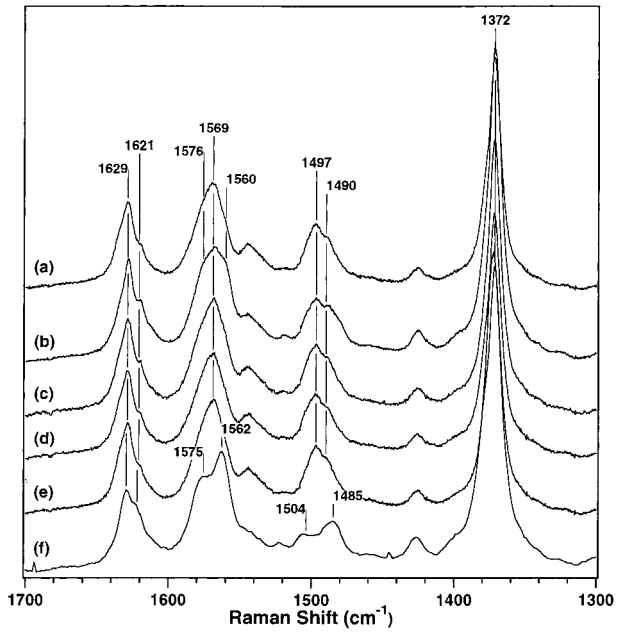

FIGURE 5: Resonance Raman spectra of ferric (a) wild-type, (b) S35K, (c) S35A, (d) Q176E, (e) Q176A, and (f) S35K/Q176E HRPs at pH 7.0 by 406.7 nm excitation. Laser power, 5 mW; accumulation time, 3 min; enzyme concentration, 30 μM.

investigated and compared with those of ARP by various spectroscopies.

CD Spectra of HRP Mutants. To assess the mutational effects on the secondary structure of HRP, we examined the CD spectrum in the near-UV region. The five HRP mutants exhibited analogous spectral patterns, which were indistinguishable from that of wild-type HRP[3] (data not shown). Table 3 collects the α-helical contents of the wild-type and mutant HRPs calculated from eq 1. The α-helical contents of the mutants were in fairly good agreement with that of the parent enzyme. This result together with the similarities of the UV−visible absorption spectra of the mutants to that of the wild-type enzyme (data not shown) confirms that all the mutants were properly refolded as wild-type HRP.

Resonance Raman Spectra of HRP Mutants. The coordination and oxidation states of the heme in the ferric state were investigated by resonance Raman (RR) spectra with 406.7 nm excitation (Figure 5). The Raman lines in the ν_3 region for both wild-type and single mutant HRPs were detected at 1490 and 1497 cm^{-1}, which show 6- and 5-coordinated high-spin forms of the heme, respectively (*30*).

[3] Since both wild-type and mutant HRPs are not glycosylated due to expression from *Escherichia coli*, wild-type HRP, instead of native HRP, was utilized as a reference for the structural and catalytic properties of the HRP mutants.

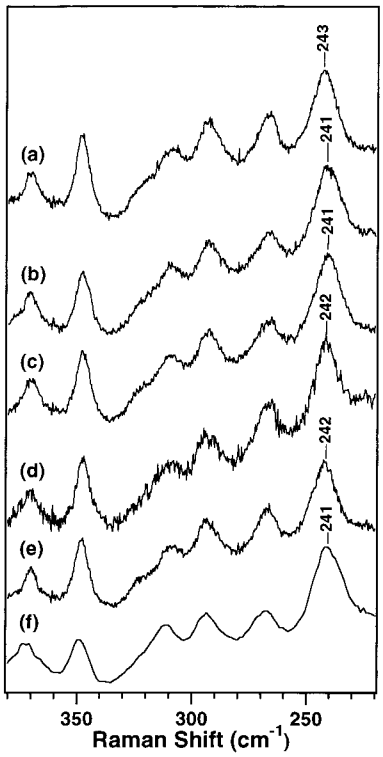

FIGURE 6: Resonance Raman spectra of ferrous (a) wild-type, (b) S35K, (c) S35A, (d) Q176E, (e) Q176A, and (f) S35K/Q176E HRPs at pH 7.0 by 441.6 nm excitation. Laser power, 5 mW; accumulation time, 6 min; enzyme concentration, 30 μM.

Thus, the coordination and spin states of the heme group in the single mutants were similar to those of wild-type enzyme. On the other hand, the S35K/Q176E mutant showed the Raman lines at 1485 and 1504 cm^{-1}, both of which have been assigned to 6-coordinated high- and low-spin forms of the heme, respectively (*30*). The transition of the coordination and spin states was also encountered for some HRP mutants having the mutations at the distal residues, in which the polarity in the distal cavity is perturbed (*30*). The double mutation in this study would, therefore, also affect the polarity of the distal cavity, resulting in the changes of the coordination and spin states. As previously reported (*11*), however, such changes in the heme group of the double mutant do not seriously impair the peroxidase activity.

The coordination state of the proximal His to the heme iron was also examined by RR spectra in the low-frequency region of ferrous HRPs with 441.6 nm excitation (Figure 6). The RR spectrum of the reduced wild-type HRP is characterized by the presence of a strong line at 243 cm^{-1} assigned to the stretching mode between the ferrous heme iron and the anionic proximal imidazole (His170) (*31*). The Fe^{2+}−His stretching lines of the mutants were detected at almost the same position (241 or 242 cm^{-1}) as that of the parent enzyme, which was much higher than that of myoglobin having a neutral proximal His (*32*). Therefore, the anionic property of the proximal His was not influenced by the mutations at positions 35 and 176.

^{1}H NMR Spectra of HRP Mutants. The electronic state of the heme cofactor was explored by ^{1}H NMR spectroscopy. Figure 7 displays paramagnetic ^{1}H NMR spectra of the ferric wild-type and mutant enzymes in 90% H_2O/10% ^2H_2O at 17.0 °C. For wild-type enzyme, four peaks assigned to the heme peripheral methyl groups were observed at 84, 76, 72,

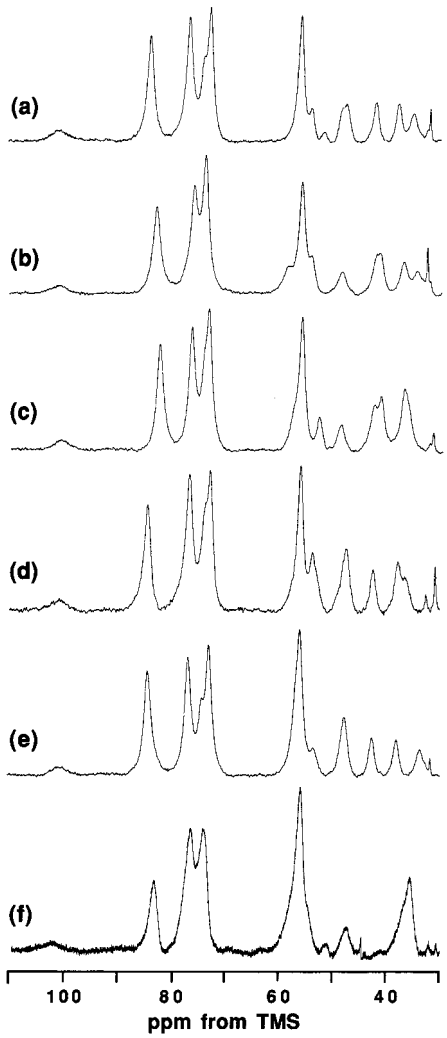

FIGURE 7: ^{1}H NMR spectra in the hyperfine-shifted region of the resting states of (a) wild-type, (b) S35K, (c) S35A, (d) Q176E, (e) Q176A, and (f) S35K/Q176E HRPs in 90%H_2O/10%^2H_2O sodium phosphate buffer, pH 7.0 at 17.0 °C.

and 56 ppm (5-, 1-, 8-, and 3-methyl group, respectively) (*33*). All the ferric mutants exhibited similar hyperfine-shifted resonances from the methyl groups of the porphyrin ring to the parent enzyme. The average position of the four methyl resonances was 72 ppm for wild-type HRP, which was not altered by the mutations at positions 35 and 176. The broad resonance for $N_\delta H$ of the proximal His (His170) (*33*) observed at 101 ppm in the spectra of all the mutants was also found at the same position as that of the parent enzyme. However, some minor but significant spectral changes were found in the region from 30 to 50 ppm for the double mutant, in which the proton signals from heme propionate and vinyl groups were detected. These spectral changes suggest the introduction of the two charged residues would induce some significant structural perturbations in the heme substituents, but the structural changes in the mutants would be small, compared with those of our previous distal HRP mutants, N70V (Asn70 → Val) and N70D (Asn70 → Asp) mutants (*6*).

The heme environmental structure was investigated by ^{1}H NMR spectra of cyanide-ligated HRPs. Figure 8 (dashed line) depicts the hyperfine-shifted region of cyanide-ligated wild-type and mutant HRPs in 90% H_2O/10% ^2H_2O at 17.0 °C. Although the single amino acid substitutions induced a few spectral changes,[4] the spectral pattern of the single mutants resembled that of wild-type HRP. In the high-field region, three resonances were clearly observed at −5.8, −7.2, and −31.1 ppm in the spectrum of the wild-type enzyme (data not shown), which are assignable to Arg38 $C_\beta H$, Arg38 $C_\delta H$, and proximal His $C_\epsilon H$, respectively (*34*). These chemical shifts were also insensitive to the single mutations. On the other hand, the double mutation caused substantial spectral changes as shown in Figure 8(f), corresponding to those in the ferric form. The introduced charged residues in the S35K/Q176E mutant, Lys35 and Glu176, might interact electrostatically with other neighboring residues, resulting in the heme environmental changes. Assignments for the specific resonances of the mutant enzymes are summarized in Table 4.

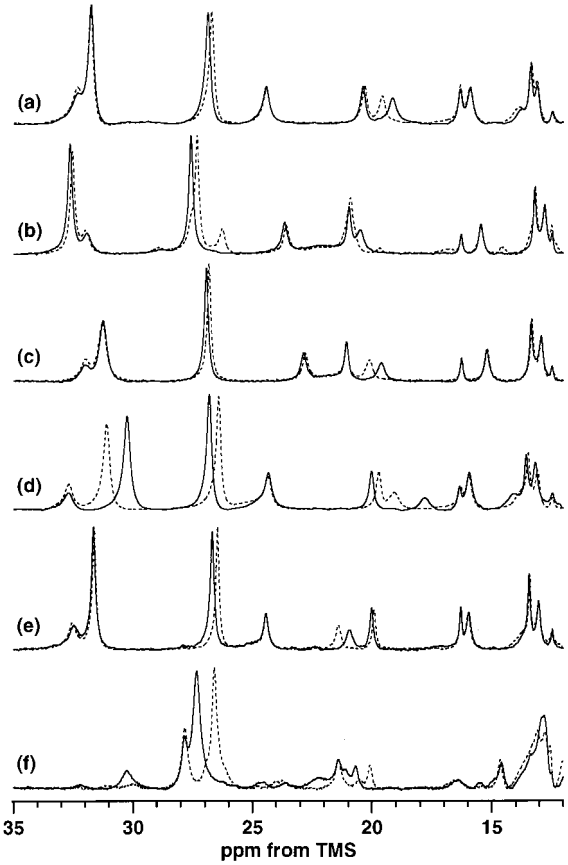

FIGURE 8: ^{1}H NMR spectra in the low-field regions of cyanide-ligated (a) wild-type, (b) S35K, (c) S35A, (d) Q176E, (e) Q176A, and (f) S35K/Q176E HRPs before (dashed line) and after (solid line) addition of luminol (4 mM) in 90% H_2O/10% ^2H_2O sodium phosphate buffer, pH 7.0 at 17.0 °C.

Structural changes in the heme environment of the HRP mutants upon addition of luminol (4 mM) were followed by ^{1}H NMR spectroscopy (Figure 8, solid line; Table 4).[5] Addition of luminol to the ARP-type HRP mutants, S35K, Q176E, and S35K/Q176E, induced significant deviations of the resonances not only from the heme group but also from the amino acid residues near the heme, whereas in the

[4] The S35K and S35K/Q176E mutants were not spectroscopically homogeneous. Since the purity of the mutant enzymes is confirmed on SDS−PAGE, the minor peaks might arise from different conformers of the mutants. Such a heterogeneity has been encountered for NMR spectra of recombinant peroxidases (*40*).

Table 4: Chemical Shifts (ppm from TMS) and Assignments of Heme and Amino Acid Protons of Cyanide-Ligated Wild-Type, S35K, S35A, Q176E, Q176A, and S35K/Q176E HRPs at 17.0 °C[a]

assignment	wild-type	S35K	S35A	Q176E	Q176A	S35K/Q176E
heme 8-CH_3	31.8	32.5 (+0.1)	31.3	31.1 (−0.8)	31.6 (+0.1)	27.8
heme 3-CH_3	26.7 (+0.2)	27.3 (+0.3)	26.8 (+0.2)	26.4 (+0.4)	26.5 (+0.2)	26.6 (+0.7)
heme 4-H_α	20.4 (+0.1)	20.9 (+0.1)	21.1	19.7 (+0.3)	19.9 (+0.1)	20.1 (+0.6)
heme 7-H_α	19.6 (−0.5)	20.8 (−0.3)	20.1 (−0.5)	19.1 (−1.3)	21.4 (−0.5)	20.5 (+0.7)
His42 $N_\epsilon H$	32.3	32.0 (−0.1)	32.0	32.7	32.5	ND
His42 $N_\delta H$	16.3	16.3	16.3	16.3 (+0.1)	16.3	16.5
His42 $C_\epsilon H$	13.4	13.2	13.3 (+0.1)	13.5 (+0.1)	13.4	13.1
His170 $C_\beta H_1$	24.4	23.6 (+0.1)	22.8 (+0.1)	24.3	24.4	21.4
His170 $C_\beta H_2$	15.9	15.5	15.2	16.0 (−0.1)	16.0	14.7
His170 $C_\epsilon H$	−31.2	−29.9 (−0.3)	−28.4	−30.9 (+0.6)	−31.3	−18.1 (+0.1)
Arg38 $C_\beta H$	−5.9	−5.4	−5.2 (+0.1)	−5.8	−5.9 (+0.1)	−7.9 (−0.3)
Arg38 $C_\delta H$	−7.3	−7.4 (−0.1)	−7.2	−7.1 (+0.5)	−7.4	−11.2

[a] The value in parentheses denotes the shift upon addition of luminol (4 mM). ND denotes not determined.

Table 5: Kinetic Parameters[a] of Oxidation for Hydroquinone, ABTS, and Luminol of Wild-Type, S35K, S35A, Q176E, Q176A, and S35K/Q176E HRPs and ARP

	luminol			hydroquinone			ABTS		
peroxidase	K_m[b]	V_{max}[c]	V_{max}/K_m[d]	K_m[e]	V_{max}[f]	V_{max}/K_m[g]	K_m[e]	V_{max}[f]	V_{max}/K_m[g]
wild-type	3.50	0.194	55.4	319	483	1.51	317	19.3	60.9
S35K	2.28	0.164	71.9	357	356	0.997	355	37.3	105
S35A	2.92	0.171	58.6	326	409	1.25	613	37.8	61.7
Q176E	4.01	0.172	42.9	360	423	1.18	365	13.3	36.4
Q176A	4.01	0.141	35.2	354	478	1.35	428	23.7	55.4
S35K/Q176E	1.45	0.152	105	736	80.9	0.110	339	21.5	63.4
ARP	0.143[h]	3.48[h]	24300[h]	969	273	0.282	102	296	2900

[a] Error is less than 10%. [b] mM. [c] ΔA_{500}·nM^{-1}(heme)·min^{-1}. [d] ΔA_{500}·nM^{-1}(heme)·min^{-1}·mM^{-1}. [e] μM. [f] μM·min^{-1}. [g] min^{-1}. [h] The final concentration of ARP (1 nM) in the reaction is different from that of HRPs (20 nM).

spectrum of wild-type HRP the signals from the 3-methyl and 7-propionate of the heme were slightly affected.[6] Since the negative control mutants (S35A and Q176A) exhibited almost similar ^{1}H NMR spectra to wild-type HRP,[7] the spectral changes in the ^{1}H NMR spectra of the S35K, Q176E, and S35K/Q176E mutants can be attributable to the introduction of the charged residue into the heme environment, and the charged residues at the positions 35 and 176 would interact with polar functional groups of luminol.

Peroxidase Activities under Steady-State Conditions. To assess the oxidation activity for luminol in the ARP-type HRP mutants, we examined the kinetics of luminol oxidation under steady-state conditions. The kinetic parameters (K_m and V_{max}) of wild-type HRP, mutant HRPs, and ARP are compiled in Table 5. The K_m value of ARP was depressed ~18-fold, and the V_{max} value was enhanced ~25-fold, leading to the catalytic efficiency (V_{max}/K_m) of ARP being ~450-fold higher than that of wild-type HRP. Although none of the HRP mutants showed such a remarkable increase in V_{max}/K_m as observed for ARP, a slight but significant increase in V_{max}/K_m was detected for the S35K and S35K/Q176E mutants. The S35K and S35K/Q176E mutants exhibited 1.5- and 2-fold higher catalytic efficiency (V_{max}/K_m) than wild-type HRP, respectively. The increase in V_{max}/K_m of both HRP mutants was achieved by the decrease in the K_m value, which reflects higher binding affinity for luminol. While introduction of the negatively charged Glu residue at position 176 into the S35K mutant (S35K/Q176E double mutant) increased the oxidation activity for luminol, the single mutation of Gln176 to Glu did not improve it. Thus, the negative charge at the position 176 can form effective interactions for the binding of luminol in the presence of the positive charge at position 35. In the absence of the positive charge, however, the interactions between the Glu residue at position 176 and the positive charge on the substituent of luminol cannot contribute to the stable binding of luminol.

The oxidation activities for hydroquinone and ABTS were also measured to reveal substrate specificity of the HRP mutants. These substrates are different types of reducing agents in that hydroquinone donates both a proton and an electron to the enzyme, like luminol, whereas ABTS donates only an electron (*6*). For the hydroquinone oxidation, a large decrease in V_{max}/K_m was detected in the S35K/Q176E mutant. The characteristic decreased V_{max} and increased K_m values in the double mutant were shared with those in ARP, which showed a 3-fold increase in K_m and a 1.8-fold decrease in V_{max}, compared with wild-type HRP. The oxidation activities

[5] We tried to examine K_d values for luminol by ^{1}H NMR spectroscopy to interpret the spectral changes upon addition of luminol in the ^{1}H NMR spectra and to estimate the difference in affinity for luminol between the HRP mutants quantitatively. The low solubility of luminol, however, prevented us from determining the K_d value. We also tried to utilize UV−visible spectroscopy to estimate the K_d value. Unfortunately, however, the overlap of the absorbance of luminol (λ_{max} = 352 nm) to that of the Soret band in HRP did not allow us to decide the K_d value.

[6] The deviation of the resonance from the 3-methyl group of the heme was not clear in the ^{1}H NMR spectrum of native HRP (Figure 3). The absence of glycosylation in wild-type HRP might have some effects on the spectral changes induced by the binding of luminol.

[7] On the basis of the X-ray crystal structure of HRP, the side chains of Ser35 and Gln176 form a hydrogen bond with 6- and 7-propionates of the heme, respectively (*23*). Although the hydrogen bonds between heme propionate and protein matrix have been considered to be crucial for catalytic activities and structural maintenance around the heme prosthetic group (*41*), the present results from the S35A and Q176A mutants clearly showed that the contribution of these hydrogen bonds to the catalytic and structural properties of HRP was rather small.

Table 6: Elementary Reaction Rates[a] ($M^{-1}\cdot s^{-1}$) of Wild-Type, S35K, S35A, Q176E, Q176A, and S35K/Q176E HRPs and ARP

		luminol		guaiacol	
peroxidase	$k_1/10^7$	$k_2/10^6$	$k_3/10^4$	$k_2/10^6$	$k_3/10^5$
WT	1.3	1.7	4.2	5.0	2.9
S35K	0.94	2.1	6.0	4.7	2.2
S35A	1.1	2.6	4.7	7.5	3.2
Q176E	1.3	1.4	3.7	4.3	2.2
Q176A	1.1	1.5	3.3	4.4	2.1
S35K/Q176E	0.31	1.7	8.6	1.8	1.1
ARP	0.75	4.7	ND[b]	4.2	ND[b]

[a] Error is less than 10%. [b] Not determined due to instability of ARP compound II at neutral pH.

for hydroquinone of the S35K and Q176E mutants were moderately depressed.

In the ABTS assay, ARP exhibited 15-fold increased V_{max} and 3-fold decreased K_m values, resulting in enhancement of the V_{max}/K_m by ~50-fold, relative to wild-type HRP. While the S35K mutant also showed an increase in V_{max}/K_m by a factor of 1.7, that value was decreased in the Q176E mutant. On the other hand, the double mutation did not change the oxidation activity for ABTS.

By inspection of Table 5, the S35K and S35K/Q176E mutants displayed similar propensities of K_m and V_{max} to ARP for the substrates used in this study. Although the changes in the kinetic parameters of the HRP mutants, relative to wild-type HRP, were much smaller than those in ARP, the observed changes in the S35K and S35K/Q176E mutants are significant. Thus, it can be safely concluded that the charged residues in the vicinity of the heme can contribute to enhancement of the oxidation activity for luminol, though the contribution might not be so important.

Elementary Reaction Rates in the Catalytic Cycle. To gain further insights into the catalytic activities of the ARP-type HRP mutants, elementary reaction rates in the catalytic cycle were measured with a stopped-flow spectrophotometer. The elementary reaction rates for the mutant and parent enzymes are listed in Table 6. Although the single amino acid substitution of Ser35 and Gln176 did not significantly affect the formation rate of compound I (k_1), the double mutation depressed the reaction rate with H_2O_2, whose characteristics were shared with ARP.

The reduction rates of compounds I (k_2) and II (k_3)[8] were determined using luminol or guaiacol as a reductant. Although the reaction rates of the HRP mutants did not differ so prominently from those of wild-type HRP, the k_2 values of the S35A mutant for both luminol and guaiacol were 1.5-fold increased (Table 6). For the k_3 process, it is notable that the k_3 values for luminol of the S35K and S35K/Q176E mutants were 1.5- and 2-fold improved, respectively, relative to that of wild-type HRP. The increase in the k_3 value for luminol has also been expected for ARP (*5*), though we could not measure the k_3 value of ARP due to the instability of ARP compound II at neutral pH (*10*). On the other hand, the Q176E mutant did not show any substantial changes in the k_2 and k_3 values for luminol.

[8] Saturation kinetics are sometimes observed in the reaction of compound II, which makes it difficult to estimate exact reaction rates (*42*). In this study, the k_3 value was obtained as the second-order rate constant from the linear part of the rate vs [substrate] profile.

Table 7: Reduction Potentials (mV) of Compounds I and II of Wild-Type, S35K, S35A, Q176E, Q176A, and S35K/Q176E HRPs and ARP

peroxidase	E_0'(compound I/compound II)	E_0'(compound II/ferric)
wild-type	900 ± 2	864 ± 0
S35K	910 ± 3	891 ± 1
S35A	923 ± 4	863 ± 1
Q176E	898 ± 2	873 ± 1
Q176A	904 ± 1	855 ± 1
S35K/Q176E	ND[b]	ND
ARP[a]	915	982

[a] Reference *10*. [b] ND denotes not determined (see Results and Discussion).

Reduction Potentials of Compounds I and II. One of the factors determining catalytic activities of peroxidase is the reduction potential of active intermediate species (*12*). As summarized in Table 7, the reduction potential of ARP compound II is much higher (more than 100 mV) than that of wild-type HRP, while the increase in the reduction potential of ARP compound I is confined to 15 mV. The single mutants, S35K and Q176E, also displayed higher reduction potentials of compound II by 27 and 9 mV than wild-type enzyme, respectively. Since the mutant compound II of the S35K/Q176E mutant was very unstable to being easily reduced back to the ferric resting state, the prominent increase in the reduction potential of compound II was suggested. Unfortunately, however, the close similarity of the UV−visible spectra between the resting state and the equilibrated state after the oxidation by iridate prevented us from estimating the reduction potential of mutant compound II.

The reduction potential of compound II is one of the key factors to affect the V_{max} value under steady-state conditions, since a rate-determining step for the catalytic cycle of HRP is reduction of compound II to the ferric resting state (Table 6). As indicated in our previous study (*6*), the high reduction potential of compound II in peroxidases corresponds to the large V_{max} value. The high reduction potential of ARP compound II can, therefore, be responsible for the enhanced V_{max} value for luminol oxidation in ARP (Table 7). For the present ARP-type HRP mutants, however, the V_{max} values for luminol oxidation were depressed despite the increase in the reduction potentials of their compounds II (Table 5). Thus, the decreased V_{max} values of the ARP-type HRP mutants cannot be attributed to the changes of the redox potential. One of the possible factors is the depression of proton abstraction from the substrate. Some HRP mutants lacking the distal histidine residue exhibited the depressed proton abstraction rate, showing decreased V_{max} (*35, 36*). Enhanced polarity in the heme environment would be another factor to decrease the V_{max} (*37, 38*). Although we could not determine the primary factor to decrease the V_{max}, it can be concluded that the acceleration effect of the higher redox potential is canceled by perturbations of other factors.

Luminol Binding Site in ARP-like Mutants and Effects of Mutations on Oxidation Activity. In the ARP-like HRP mutants, addition of luminol induced some significant changes in the ^1H NMR spectra of the cyanide adducts, which clearly indicates that the newly introduced charged residues in HRP, Lys35 and Glu176, interact with luminol in the vicinity of the heme. The slight but significant increase in V_{max}/K_m for the luminol assay was observed in the S35K

and S35K/Q176E mutants, supporting the significant contribution of the newly formed electrostatic interactions to the high-affinity binding of luminol to the HRP mutants. However, the observed spectral changes in the ARP-like HRP mutants did not coincide with those in ARP, and the enhancement of the luminol oxidation activity was not so prominent. Thus, the interactions between the charged residues and luminol in the mutants might be different from those in ARP and/or some structural factors in HRP might offset the effective interactions formed by the newly introduced amino acid residues.

One of the structural factors differentiating HRP from ARP is structural differences in the distal site residues. While the main chain structure in the distal cavity is conserved between ARP and HRP, the orientations of the distal residues in ARP are different from those in HRP. For instance, the orientations of the imidazole ring of the distal His and the guanidinium group of the distal Arg in ARP are apparently distinguished from those in HRP (*22*, *23*). Since the distal His and Arg play crucial roles in the reaction mechanism of substrate oxidation, the subtle orientations of these distal residues might be essential to the oxidation activity for luminol.

Another notable structural difference in the heme cavity between ARP and HRP is phenylalanine (Phe) residues. While no Phe residues are located at the luminol binding site of ARP, three Phe residues (68, 142, 179) at the heme periphery are supposed to be located at the substrate binding site in HRP (*22*, *23*). The steric hindrance and hydrophobicity of the Phe residues would hamper the binding of luminol to the binding site formed by newly introduced amino acid residues in the ARP-like HRP mutants. Additional mutations of some of these Phe residues to nonaromatic and less bulky amino acid residues in HRP would, therefore, mimic the binding site for luminol in ARP more accurately, which might further promote luminol oxidation.

In summary, we proposed that the binding site for luminol in ARP is located near the 7-propionate and 8-methyl groups of the heme. To enhance the luminol activity of HRP, we have prepared ARP-type HRP mutants (S35K, Q176E, and S35K/Q176E), in which one or two charged residues in the putative binding site for luminol were introduced. Addition of luminol to the HRP mutants induced prominent changes in the resonance positions from heme environmental residues as well as from the heme group in the ^{1}H NMR spectra, suggesting that luminol is bound near the heme by electrostatic interactions between luminol and the introduced charged residue. Although the luminol activity of the ARP-type HRP mutants was not so high as that of ARP, the slight but significant increase in the oxidation activity for luminol was observed in the S35K and S35K/Q176E mutants. The present study showed that the positively charged residue near the 7-propionate and 8-methyl groups of the heme would be important to luminol oxidation, but other interactions should also be taken into consideration to create a specific binding site for luminol and enhance the luminol activity as observed for ARP.

ACKNOWLEDGMENT

Dr. Teruo Amachi (Suntory Ltd., presently Kyoto University) is greatly appreciated for the preparation of ARP. We are grateful to Prof. Teizo Kitagawa (Institute for Molecular Science) for kind permission to use the resonance Raman observing system. We are also thankful to Dr. Satoshi Takahashi (Kyoto University) for technical assistance with the resonance Raman experiments and critical reading of the manuscript.

REFERENCES

1. Dolphin, D., Forman, A., Borg, D. C., Fajer, J., and Felton, R. H. (1971) *Proc. Natl. Acad. Sci. U.S.A. 68*, 614−618.
2. Campa, A. (1991) in *Peroxidases in Chemistry and Biology* (Everse, J. E., Everse, K. E., and Grisham, M. B., Eds.) Vol. II, pp 25−50, CRC Press, Boca Raton.
3. Thorpe, G. H. G., and Kricka, L. J. (1986) *Methods Enzymol. 133*, 331−353.
4. Kricka, L. J., Cooper, M., and Ji, X. (1997) *Anal. Biochem. 240*, 119−125.
5. Akimoto, K., Shinmen, Y., Sumida, M., Asami, S., Amachi, T., Yoshizumi, H., Seaki, Y., Shimizu, S., and Yamada, H. (1990) *Anal. Biochem. 189*, 182−185.
6. Nagano, S., Tanaka, M., Ishimori, K., Watanabe, Y., and Morishima, I. (1996) *Biochemistry 35*, 14251−14258.
7. Tanaka, M., Ishimori, K., Mukai, M., Kitagawa, T., and Morishima, I. (1997) *Biochemistry 36*, 9889−9898.
8. Paul, K. G., Theorell, H., and Akesson, A. (1953) *Acta Chem. Scand. 7*, 1284−1287.
9. Chen, Y. H., Yang, J. T., and Martinez, H. M. (1972) *Biochemistry 11*, 4120−4131.
10. Farhangrazi, Z. S., Copeland, B. R., Nakayama, T., Amachi, T., Yamazaki, I., and Powers, L. S. (1994) *Biochemistry 33*, 5647−5652.
11. Smith, A. T., Sanders, S. A., Thorneley, R. N. F., Burke, J. F., and Bray, R. C. (1992) *Eur. J. Biochem. 207*, 507−519.
12. Hayashi, Y., and Yamazaki, I. (1979) *J. Biol. Chem. 254*, 9101−9106.
13. Boffi, A., Wittenberg, J. B., and Chiancone, E. (1997) *FEBS Lett. 411*, 335−338.
14. Veitch, N. C., Gao, Y., and Welinder, K. G. (1996) *Biochemistry 35*, 14370−14380.
15. Kjalke, M., Anderson, M. B., Schneider, P., Christensen, B., Schulein, M., and Welinder, K. G. (1992) *Biochim. Biophys. Acta 1120*, 248−256.
16. Sheard, Y., Yamane, T., and Shulman, R. G. (1970) *J. Mol. Biol. 63*, 35−48.
17. Yi, Q., Erman, J. E., and Satterlee, J. D. (1993) *Biochemistry 32*, 10988−10994.
18. Thanabal, V., de Ropp, J. S., and La Mar, G. N. (1987) *J. Am. Chem. Soc. 109*, 7516−7525.
19. La Mar, G. N., Chen, Z., Vyas, K., and McPherson, A. D. (1995) *J. Am. Chem. Soc. 117*, 411−419.
20. Behere, D. V., Gonzalez-Vergana, E., and Goff, H. M. (1985) *Biochim. Biophys. Acta 832*, 319−325.
21. Aviles, G., and Chang, C. K. (1992) *J. Chem. Soc., Chem. Commun.*, 31−32.
22. Kunishima, N., Fukuyama, K., Matsubara, H., Hatanaka, H., Shibano, Y., and Amachi, T. (1994) *J. Mol. Biol. 235*, 331−344.
23. Gajhede, M., Schuller, D. J., Henriksen, A., Smith, A. T., and Poulos, T. L. (1997) *Nat. Struct. Biol. 4*, 1032−1038.
24. Itakura, H., Oda, Y., and Fukuyama, K. (1997) *FEBS Lett. 412*, 107−110.
25. Sundaramoorthy, M., Kishi, K., Gold, M. H., and Poulos, T. L. (1997) *J. Biol. Chem. 28*, 17574−17580.
26. Veitch, N. C., Gao, Y., Smith, A. T., and White, C. G. (1997) *Biochemistry 36*, 14751−14761.
27. Ator, M. A., and Ortiz de Montellano, P. R. (1987) *J. Biol. Chem. 262*, 1542−1551.
28. Sakurada, J., Takahashi, S., and Hosoya, T. (1986) *J. Biol. Chem. 261*, 9657−9652.
29. Banci, L., Bertini, I., Bini, T., Tien, M., and Turano, P. (1993) *Biochemistry 32*, 5825−5831.
30. Smulevich, G., Paoli, M., Burke, J. F., Sanders, S. A., Thorneley, R. N. F., and Smith, A. T. (1994) *Biochemistry 33*, 7398−7407.

31. Teraoka, J., and Kitagawa, T (1981) *J. Biol. Chem. 256*, 3969−3977.
32. Kitagawa, T., Nagai, K., and Tsubaki, M. (1979) *FEBS Lett. 104*, 376−378.
33. La Mar, G. N., de Ropp, J. S., Smith, K. M., and Langry, K. C. (1980) *J. Biol. Chem. 255*, 6646−6652.
34. Chen, Z., de Ropp, J. S., Hernandez, G., and La Mar, G. N. (1994) *J. Am. Chem. Soc. 116*, 8772−8783.
35. Newmyer, S. L., and Ortiz de Montellano, P. (1995) *J. Biol. Chem. 270*, 19430−19438.
36. Tanaka, M., Ishimori, K. and Morishima, I. (1996) *Biochem. Biophys. Res. Commun. 227*, 393−399.
37. Gazaryan, I. G., Doseeva, V. V., Galkin, A. G., and Tishkov, V. I. (1994) *FEBS Lett. 354*, 248−250.
38. Bujons, J., Dikiy, A., Ferrer, J. C., Banci, L., and Mauk, A. G. (1997) *Eur. J. Biochem. 243*, 72−84.
39. Morishima, I., and Inubushi, T. (1978) *J. Am. Chem. Soc. 100*, 3568−3574.
40. Satterlee, J. D., Alam, S. L., Mauro, J. M., Erman, J. E., and Poulos, T. L. (1994) *Eur. J. Biochem. 224*, 81−87.
41. Adak, S., and Banerjee, R. K. (1998) *Biochem. J. 334*, 51−56.
42. Critchlow, J. E., and Dunfold, H. B. (1972) *J. Biol. Chem. 247*, 3703−3713.

BI9907328